MODELLING OF GLASS REFINING KINETICS PART 2. BUBBLE DISTRIBUTION MODELS AND METHODS OF MEASUREMENT OF REFINING PROPERTIES

JAROSLAV KLOUŽEK, LUBOMÍR NĚMEC

Laboratory of Inorganic Materials
Joint Workplace of the Institute of Inorganic Chemistry of the Academy of Sciences of the Czech Republic and the Institute of Chemical Technology in Prague, Technická 5, 166 28 Prague, Czech Republic

E-mail: klouzekj@vscht.cz

Submitted May 19, 2003; accepted September 4, 2003

Keywords: Glass melt, Bubble, Distribution, Models.

The contemporary approach to modeling of the glass melting process involves presentation of concentration fields of inhomogeneities in a modeled melting space. In addition to kinetics of single inhomogeneities in the melt, their distribution in the space is therefore calculated. This work presents three distribution models necessary for modeling refining process and glass quality control: The distribution model of components of oxidation-reduction reactions and two models of particle distribution (bubbles, solid particles) in the melting space. The model applicability is discussed and examples of model applications are presented. The methods and procedures of data acquisition for refining models are described.

INTRODUCTION

The real glass melting facility involves a non-isothermal space with continuous melt flow. A multitude of bubbles are entering the space by boundaries (glass batch, surface of refractory materials) or are formed in the melt. Bubbles are reacting with the melt according to relations presented in [1] and distributed in the space by glass flow and buoyancy force. As a result of this process, the bubble concentration field evolves in the space. The shape and intensity of the bubble concentration field gives evidence of the bubble removing from glass. The high concentrations of bubbles in the melt influence the melt properties as are average melt density, viscosity and thermal conductivity, consequently the temperature and velocity fields of the melt, as well as resulting bubble concentration field, are result of mutual impact of melt and bubbles. The bubble growth or dissolution is mostly influenced by the concentration field of oxidation-reduction components of refining agent reactions in the space. The resulting concentration field of oxidation-reduction components in the real melting space is mostly determined by the temperature distribution, however, the component transport by the melt convection and by diffusion play also their role. Probably also bubbles influence the redox concentration distribution by their extraction ability.

This work presents three distribution models of components and particles in the glass melting space:

1. The distribution model of oxidation-reduction species.
2. The distribution model of particles (solid particles, bubbles) based on particle tracing (the model of particle representatives).
3. The distribution model of particles (solid particles, bubbles) based on flow of monodisperse particle phases through the melting space (the convective model).

Both complete and simplified models of single bubbles, described in Part 1 [1], are applicable in the distribution model No.2, while only the simplified model is usable in the convective model No.3. The convective model should be applied when examining the bubble impact on glass flow in the space.

THEORETICAL

Distribution of oxidation-reduction species in the melting space

The general formal equation expressing the oxidation-reduction behavior of refining agents and transition metals is given by:

$$4/b\ Me^{(a+b)+}\ (l) + 2O^{2-}\ (l) \leftrightarrow 4/b\ Me^{a+}\ (l) + O_2\ (g,l) \quad (1)$$

where b is the number of transferred electrons.

For the sulfate equilibrium is valid:

$$2SO_4^{2-}(l) \leftrightarrow 2SO_2\,(g,l) + O_2\,(g,l) + 2O^{2-}\,(l) \qquad (2)$$

If two or more oxidation-reduction pairs are present in the melt, oxygen is shared by all pairs.

As the reactions are fast, the chemical equilibrium sets almost instantly in the melt. For the former equations and low concentrations of oxidation-reduction species in melt, we have:

$$K_{Me} = \frac{c_{Me^{a+}}^{4/b}\, c_{O_2}}{c_{Me^{(a+b)+}}^{4/b}\left[O^{2-}\right]^2};\quad K_{SO_4^{2-}} = \frac{c_{SO_2}^2\, c_{O_2}\left[O^{2-}\right]^2}{c_{SO_4^{2-}}^2} \qquad (3)$$

where c_i are the appropriate concentrations of ions related to the standard state and $[O^{2-}]$ is the oxygen ion concentration in the melt of given composition (considered constant when equilibrium of chemical reactions shifts). The calculation of chemical equilibrium at constant temperature and in the quiescent glass melt provides the potential refining ability of the melt as is obvious from figure 5 in Part 1 of this work [1].

Under real conditions of non-isothermal melting and glass flow, the mass transfer of oxidation-reduction species takes place through their diffusion and convection. Consequently, the equilibrium of oxidation-reduction reactions is continually shifted when changing conditions. In the steady state, the chemical equilibrium given by equations (1-2), are attained and diffusive-convective relations for single reaction components are simultaneously valid [2].

Considering the first oxidation-reduction equation, we get:

$$\begin{aligned} D_{Me^{(a+b)+}}\nabla^2 c_{Me^{(a+b)+}} - \mathbf{v}\nabla c_{Me^{(a+b)+}} + R_{Me^{(a+b)+}} &= 0 \\ D_{Me^{a+}}\nabla^2 c_{Me^{a+}} - \mathbf{v}\nabla c_{Me^{a+}} + R_{Me^{a+}} &= 0 \\ D_{O_2}\nabla^2 c_{O_2} - \mathbf{v}\nabla c_{O_2} + R_{O_2} &= 0 \end{aligned} \qquad (4\text{-}6)$$

where D_i are the appropriate diffusion coefficients, $\mathbf{v}$ is the vector of glass velocity and R_i are the appropriate chemical sources, resulting from shifting the chemical equilibrium of equation (1), and bound by the reaction stoichiometry:

$$R_{Me^{(a+b)+}} = -R_{Me^{a+}} = -\frac{b}{4}R_{O_2} \qquad (7)$$

Numerical solution of equations (4-7) gives the distribution of oxidation-reduction components, i.e. as well distribution of the value of m_{ib} (O_2, SO_2) in the space (m_{ib} see equations (8-9) in Part 1). The influence of bubbles on the component distribution is not involved in this model. Figure 1 presents the oxygen distribution in the model melting space calculated by using the described model.

High bubble concentrations in the melting space influence also the distribution of oxidation-reduction components in the melt as shoved preliminary calculations [3]. To take into account this fact, simultaneous calculations of temperatures, velocities and concentration fields of oxidation-reduction species as well as bubble concentration field in the space are necessary. The special model of single bubble behavior was proposed for this purpose [4]. The proposed bubble model uses equation (8) in Part 1 of this work; however, the bubble composition is considered constant with time, reflecting only the varying oxidation-reduction state of the melt.

Particle distribution and rising or settling in the particle tracing model (Model of particle representatives)

When applying the model for bubbles, the bubble trajectories are followed in the melting space. Instead of following all entering bubbles, only s.c. bubble representatives are traced [5]. It is assumed that the trajectory of the given bubble representative differs only slightly from trajectories of bubbles having sizes and starting points close to the mentioned bubble representative. Consequently, the represented bubbles find their positions on the trajectory of the bubble representative. Thus, several thousands up to tens of thousands of representative bubbles are followed instead of all entering bubbles. In the steady state, all bubbles are located on trajectories of bubble representatives and the appropriate bubble concentration field is obtained by summation of these bubbles in appropriate elementary volumes of melt. The schematic trajectory of a bubble representative presents figure 2.

Considering arbitrary bubble representative trajectory, the amount of represented bubbles is characterized by the frequency of bubbles entering the melting space. This frequency is given by the melting space output and by the bubble formation intensity.

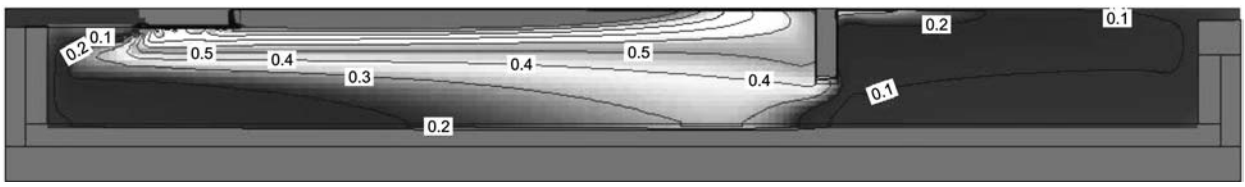

Figure 1. Oxygen distribution in a longitudinal section through the modeled melting space (mol/m^3).

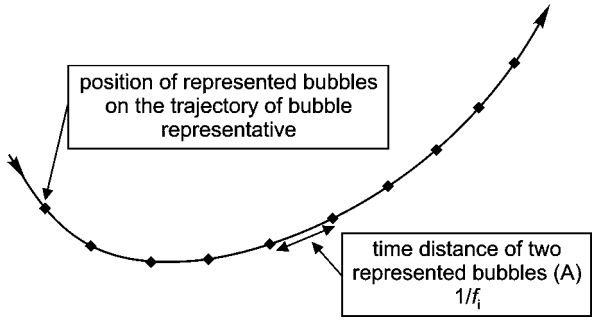

Figure 2. The schematic trajectory of a bubble representative with positions of represented bubbles in a melting space; f_i - frequency of entering of bubbles in the i-th class of bubble sizes.

As is obvious, several sources of bubbles may be considered, kinetics of bubble behavior is taken into account by applying the complete bubble kinetic model (equations (8-9)) or the simplified bubble model (equations (13) and (15)) in Part 1 of this work. Figure 3 presents the bubble concentrations in cross sections through the model-melting furnace having thickness 1 m. Both single bubble models described in Part 1, the complete and simplified ones, are applied. The results acquired by using mentioned models are similar; this fact confirms the good applicability of the simplified model for bubble distribution calculations in melting spaces.

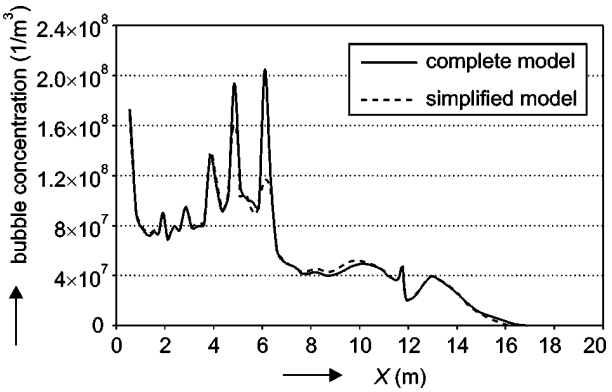

Figure 3. The bubble concentrations in cross sections through the model-melting space. Bubble tracing model. Complete model: equations (8-9) in Part 1 [1]; Simplified model: equations (13) and (15).

Particle distribution and rising or settling in the convective model

Ungan et al. have presented the convective bubble distribution model for one component bubble [6]. This paragraph presents the model of multicomponent bubble distribution in the space. Particles, i.e. bubbles enter the melting space as a new phase; they are distributed by glass convection and by their own rising due to buoyancy force. The concentration of particles is further determined by their interaction with the melt, i.e. by particle growth or shrinking. The transport of bubbles by diffusion is neglected. The governing equation valid for mass concentration of monodisperse bubbles in given point of the space has the form:

$$\frac{\partial c}{\partial \tau} = -\left[v_x \frac{\partial c}{\partial x} + v_y \frac{\partial c}{\partial y} + \left(v_z - \frac{2g\rho a^2}{9\eta} \right) \frac{\partial c}{\partial z} \right] + R \quad (8)$$

R is the bubble concentration change by their dissolution or growth and is given by:

$$R = 4\pi N_B \rho_{bub}\, a^2(\tau)\, \frac{da}{d\tau} = \frac{3C_{in}}{a_0^3}\, a^2(\tau)\, \frac{da}{d\tau} \quad (9)$$

where $da/d\tau$ is the bubble growth or dissolution rate obtainable from equations describing kinetics of behavior of single bubbles (equations (8-9) or (13) and (15) in Part 1), N_B is bubble number density in the given point, ρ_{bub} is the bubble density and C_{in} is the bubble entering concentration in the melt. For polydisperse bubbles entering the melting space, we have:

$$\begin{aligned} \frac{\partial C^{\Sigma}}{\partial \tau} = \frac{4}{3}\pi\rho_{bub} \{ & v_x \int_{a_{min}}^{a_{max}} \frac{\partial [N_B f(a)]}{\partial x}\, a^3(a_0,\tau)\, da + \\ & + v_y \int_{a_{min}}^{a_{max}} \frac{\partial [N_B f(a)]}{\partial y}\, a^3(a_0,\tau)\, da + \\ & + \int_{a_{min}}^{a_{max}} \left(v_z - \frac{2g\rho a^2(a_0,\tau)}{\partial x} \right) \frac{\partial [N_B f(a)]}{\partial z}\, a^3(a_0,\tau)\, da \} + \\ & + 4\pi\rho_{bub} N_B \int_{a_{min}}^{a_{max}} a^2(a_0,\tau)\, a(\tau)\, f(a)\, da \end{aligned} \quad (10)$$

If entering bubbles are polydisperse, the probability density function, $f(a)$, is both size and time dependent. In numerical solution of equation (10), the bubble redistribution into classes of bubble sizes is performed in every calculation step. The calculation of the bubble distribution is terminated after reaching the steady state, i.e. $\partial C^{\Sigma}/\partial\tau = 0$. At present, only the simplified model of bubble behavior, i.e. equations (13) and (15) in Part 1 are applied for the described convective distribution model.

RESULTS OF CALCULATIONS AND DISCUSSION

Bubble influence on glass properties and behavior

The volume concentration of bubbles in some areas of the melting furnace (below batch blanket, in the temperature maximum, see figure 3) is high enough to influence of the melt and consequently, the melting process. The glass viscosity increases with concentration of particles in the melt according to formula [7]:

$$\eta = \frac{\eta_0}{(1 - \vartheta)^{2.5}} \quad (11)$$

where ϑ is volume fraction of spherical particles in the liquid.

Thus, the glass viscosity in the given point of the melting space is given by temperature and bubble concentration (the influence of present solid particles is neglected).

The average glass density distinctly decreases in areas with high bubble concentrations and the arising buoyancy force competes with free convection evoked by temperature differences. If the volume fraction of bubbles in the melt is given by quantity ϑ, then the average density of the mixture melt - bubbles at constant temperature is given by:

$$\rho_b = \rho(1 - \vartheta) \tag{12}$$

where the volume fraction of bubbles is calculated by using appropriate bubble and distribution models. The calculations performed on 2D model [8,9] and preliminary calculations using model of bubble representatives in 3D space [10] have indicated the distinct impact of bubbles on glass flow in regions with high bubble concentrations. To get more realistic values of value fields, the convective distribution model should be nevertheless applied.

Figure 4 presents this situation by comparison of glass velocity fields in the central longitudinal section through the melting space for cases without and with the influence of bubble buoyancy force.

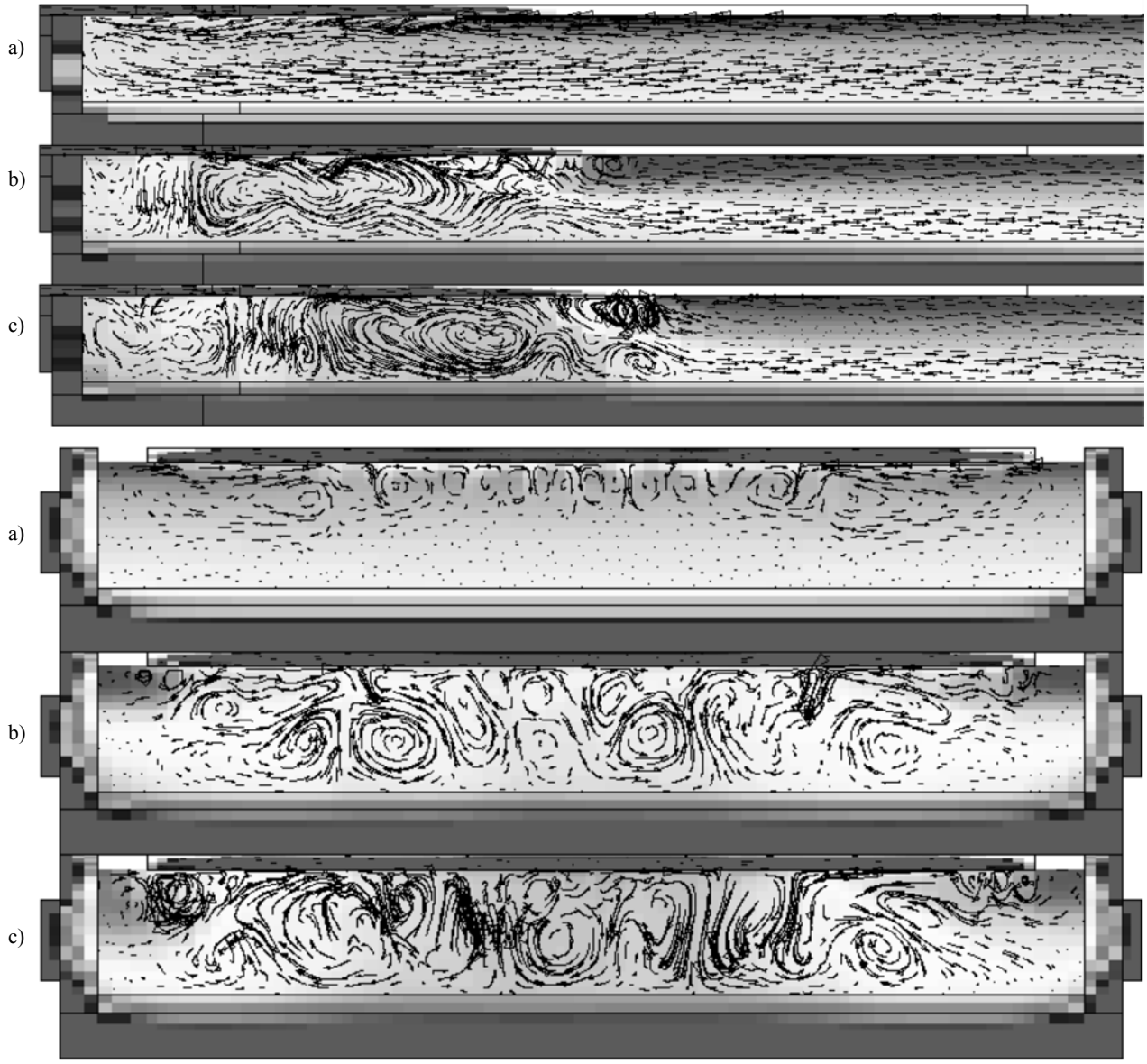

Figure 4. The flow patterns of glass melt in the model-melting space. The longitudinal and cross sections.
a) without bubble influence, b) with bubble influence (standard bubble input concentration), c) with bubble influence (ten times higher bubble input concentration).

In figure 4, parts of glass pathways corresponding to time interval 60 s are projected into YZ and central XZ planes to show flow patterns of glass. Generally, bubbles entering the space from the front of batch layer restrict the back flow of glass coming from the region of temperature maximum and bring about temperature decrease in the below batch region. On the other side, the horizontal bubble concentration gradients evoke circulation flows extending up to the furnace bottom and thus effectively stir the glass melt in vertical direction. This is also obvious from figures 4b and 4c.

Bubbles also reduce the effective heat conductivity of glass as heat conduction decreases with amount of present insulating bubbles and radiation transport is obstructed by radiation scattering on bubble surfaces. The model of bubble effect on heat transfer in melt is needed to describe refining process completely.

As already mentioned, the behavior of bubbles in a real melting space is considerably determined by the distribution model of oxidation-reduction species in the space [3]. The advanced refining model assumes therefore simultaneous solution of equations describing distribution of glass velocities, temperatures, oxidation-reduction components and bubbles in the melting space.

MEASUREMENT OF REFINING PROPERTIES

The crucial values involve kinetic and equilibrium data of single bubbles and single gases in a glass melt namely bubble growth or dissolution rates, their compositions and diffusion coefficients, solubilities and actual concentrations in the melt. While the first two groups of data are needed by the simplified bubble model, the data of single gases uses the complete model of single bubbles.

The data needed for the simplified (experimental) model described by equations (13) and (15) in Part 1 [1]

The simplified equations involve two values, which have to be acquired experimentally, namely $(da/d\tau)_D$ - the bubble growth rate at constant temperature and in the stationary state, and C - the stationary concentration of the refining gas in the bubble. The temperature dependence of both quantities should be measured to describe behavior of bubbles in the stationary state as assumes equation (15).

The measurement of bubble growth rates in glass melts needs a proper visual method working at high temperatures. The method of high temperature observation of phenomena in molten glass, video recording and image analysis, is applied for this purpose. The glass sample is inserted into a flat silica glass probe and heated to melting temperature in a laboratory furnace with observation window. To ensure the sufficiently long time period for observation of a rising bubble, two experimental arrangements are used:

- the measuring part of the silica glass cell is sufficiently high (at least ten centimeters) and the whole cell is vertically shifted during experiment to keep the rising bubble in the visual field
- the observed bubble is alternatively rising through glass in the measuring cell and inside a silica glass tube immersed in glass. The bubble is continuously pumped between both positions by pressure change in the tube. The method, called "shuttle method", is currently applied to measure $(da/d\tau)_D$. The scheme of the "shuttle method" is in figure 5.

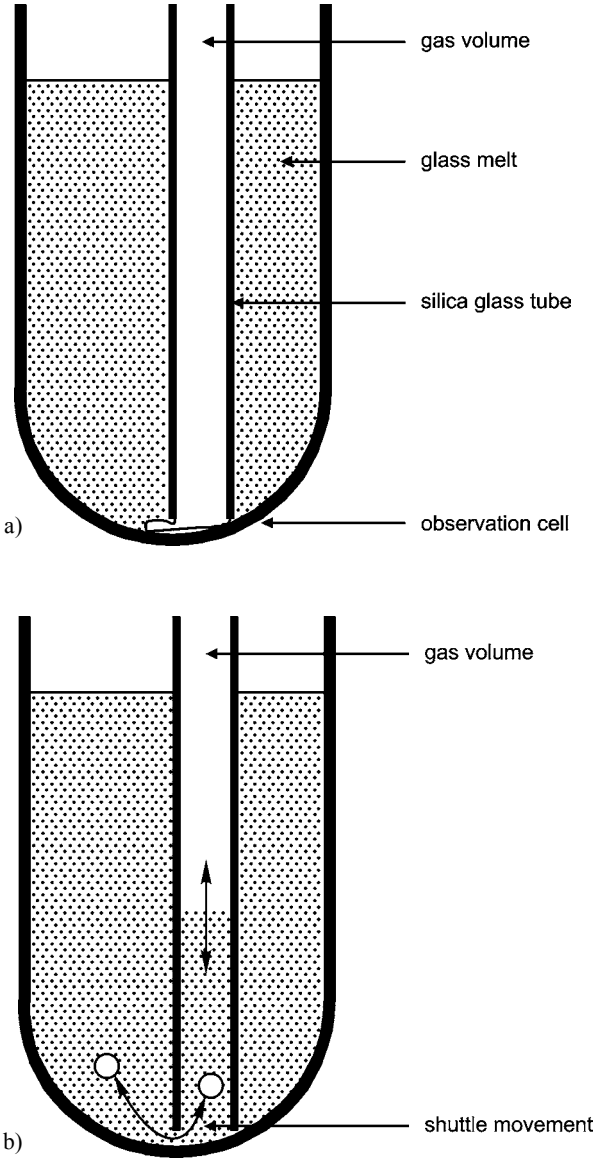

Figure 5. Scheme of the "shuttle" method for measurement of bubble growth or dissolution rate in glass melts - a) bubble preparation, b) bubble movement.

In order to ascertain the bubble composition, bubbles in cooled glass samples are analyzed, most frequently by mass spectrometry. The stationary concentration of the refining gas (value C in equation (15)) in bubbles at melting temperatures is, however, obtained with a great error, when applying bubble analysis. The high solubility of the refining gas in glass and its steep temperature dependence brigs about the rapid absorption of refining gas into glass during cooling, consequently the found values of C are too low. Nevertheless, the rapid absorption of the refining gas may be utilized to measure C. The visual observation of bubbles is advantageously used for this purpose. Bubbles of stationary composition and at given temperature are prepared in the melt and video recorded. Subsequently, temperature is abruptly decreased to the value characterized by the negligible stationary concentration of the refining gas (approximately 1200°C in commercial glass melts). The refining gas is considered as absorbed gas, the mass transfer of remaining gases during temperature drop is neglected.

The data needed for the complete model described by equations (8-9) in Part 1

If the simplified model is not precise enough or bubbles are modeled with the aim to reveal and localize the defect bubble source, the complete model of bubble behavior should be applied to follow both size and composition bubble history.

The accuracy of measurements of gas solubilities and concentrations, as well as diffusion coefficients is usually not satisfactory enough for the true representation of bubble histories. This fact leads to an idea to use - similarly as in case of the simplified model - the kinetic data of bubble behavior for acquisition of maximum scope of mentioned data. The set of differential equations describing bubble size and composition development (equations (8-9)) in Part 1 makes the theoretical base of the procedure.

These kinetic equations involve the terms $D_i^{2/3}$ (m_{ib} - m_{ia}) = $D_i^{2/3}$ (m_{ib} - $L_i p_i$). The quantity L_i is the solubility of the *i-th* gas in the melt and p_i is its partial pressure in a bubble. D_i, m_{ib} and L_i are the data necessary for bubble modeling.

Experiments with shuttling or rising bubbles provide dependences between a and τ; if the experiment is properly arranged, also the development of bubble composition may be obtained. To get the relation between the bubble composition and time, the observed bubble should be caught, taken out of the melt and analyzed after sample cooling. Taking into account the initial non-stationary stage of bubble behavior and two experimental points providing values of bubble radii, namely a_j and a_{j+1}, and the appropriate couples of partial pressures of the *i-th* gas, p_{ij}, $p_{i,j+1}$ in the bubble, the appropriate products have the form obtained from equations (8-9) after rearranging:

$$D_i^{2/3} L_i = \frac{a_{j+1} M_i}{3A(p_{ij} - p_{i,j+1})}\left[\frac{dp_{i,j+1}}{d\tau} + \frac{3p_{i,j+1}}{a_{j+1}}\frac{da_{j+1}}{d\tau} - \frac{a_j}{a_{j+1}}\frac{dp_{ij}}{d\tau} - \frac{3p_{ij}}{a_{j+1}}\frac{da_j}{d\tau}\right] \quad (13)$$

and:

$$D_i m_{ib} = \frac{a_j M_i}{3A}\frac{dp_{ij}}{d\tau} + D_i^{2/3} L_i p_{ij} + \frac{M_i p_{ij}}{A}\frac{da_j}{d\tau} \quad (14)$$

where:

$$A = \frac{0.382 RT g^{1/3} \rho^{1/3}}{\eta^{1/3}} \quad (15)$$

Equations (13) and (14) are slightly modified for water vapor as water concentration (in form OH groups) depends on the square root of p_{H_2O}.

From both equations is obvious that they are valid only when $p_{ij} \neq p_{i,j+1}$, i.e. in the non-stationary region of bubble life. Consequently, non-stationary bubbles should be measured in laboratory experiments.

While the values of a_j, a_{j+1}, p_j and p_{j+1} are the measured values, the appropriate derivatives need the substitution of experimental results by empirical functions $a = a(\tau)$ and $p_i = p_i(\tau)$.

The bubble input data

The frequency of bubbles entering the melting space is determined by laboratory experiments. When determining the frequency of bubbles coming from the glass batch, the batch is exposed to the average time-temperature regime of the batch in the real equipment. The bubble density and size distribution is ascertained from cooled samples. If N_{Bi} is the bubble number density of the i-th class of bubble sizes measured by experiment, the bubble entering frequency in the mentioned class is given by:

$$f_{iBatch} = \frac{N_{Bi} P}{\rho} \quad (16)$$

where P is the mass pull rate of the space.

When searching for secondary bubble sources, the bubble entering frequency is directly measured by appropriate experiments. The high temperature observations of bubble forming and releasing, connected with image analysis (bubble counting, bubble size determination), is mostly applied. The following figure 6 presents the sequence of high temperature images of a glass melt with a piece of refractory material, showing bubbles evolved from the material. The right part of the picture shows the establishing of the stationary rate of bubble evolution from several commercial refractory materials.

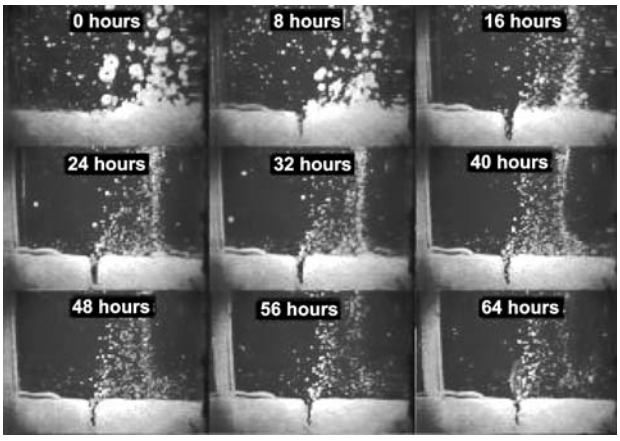

Figure 6. The sequence of high temperature images of a glass melt with pieces of refractory materials, presenting bubbles evolution from two compared materials; temperature 1200°C.

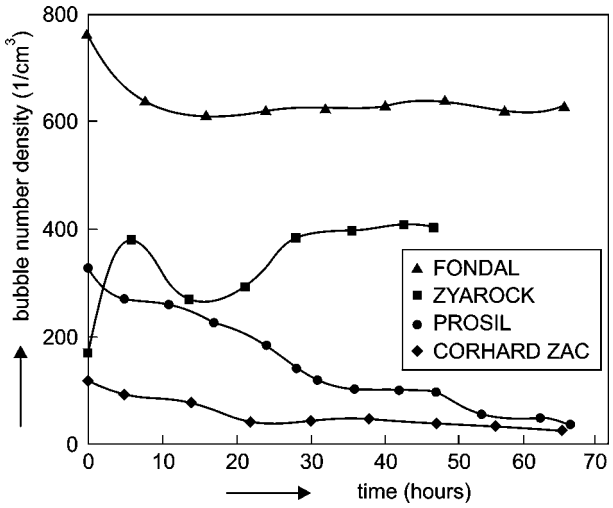

CONCLUSION

The particle distribution models help to provide a more complete picture of the industrial glass melting process. In addition, they reveal the potential mutual influence of bubble multitude and glass melt. The distribution model of oxidation-reduction species does not involve the expected extraction effect of bubbles. The bubble distribution model based on bubble representative tracing provides the bubble concentration field in the space, including actual bubble compositions, however, can not be used for calculation of mutual impact bubbles and melt. The model should be applied for the identification of defect bubble sources. The convective model is destined to perform the simultaneous calculations of bubble and melt behavior. The further development of distribution models leads to their simultaneous application. The adequate experimental methods and procedures should be developed to get data into refining models. The high temperature observations of bubble kinetics belong to the mostly used ones.

Acknowledgement

This work was supplied with the subvention by the Grant Agency of ASCR, Project No. S4032103 and by Schott Glass, Mainz, Germany.

References

1. Němec L., Kloužek J.: Ceramics-Silikáty *47*, 81 (2003).
2. Němec L., Raková M.: Ceramics-Silikáty *42*, 1 (1998).
3. Matyáš J., Němec L.: Glastechn.Ber.Glass Sci.Technol., to be published.
4. Němec L. Unpublished results.
5. Kloužek J., Matyáš J., Němec L., Trochta M., Ullrich J.: Proceedings of the 5th Conference of European Society of Glass Science and Technology, paper no. A 2-3, Czech Glass Society, Prague 1999.
6. Balkanli B., Ungan A.: Glass Technol. *37*, 164 (1996).
7. Brikman H.C.: J.Chem.Phys. *20*, 571 (1952).
8. Kloužek J, Franěk A.: Ceramics-Silikáty *45*, 70 (2001).
9. Němec L., Jiřička M., Matyáš J., Franěk A.: Ceramics-Silikáty *45*, 129 (2001).
10. Matyáš J. Němec L. Jiřička M., Franěk A.: Proceedings of the International Conference Glass in the New Millenium - Challenges and Break-through Technologies, CD ROM, Part T1.3), Amsterdam 2000.

MODELOVÁNÍ KINETIKY BUBLIN V TAVICÍM PROCESU SKEL ČÁST 2. DISTRIBUČNÍ MODELY BUBLIN A METODY MĚŘENÍ DAT

JAROSLAV KLOUŽEK, LUBOMÍR NĚMEC

Laboratoř anorganických materiálů, společné pracoviště Ústavu anorganické chemie AV ČR a Vysoké školy chemicko-technologické Praha, Technická 5, 166 28 Praha

Požadavky na současné matematické modely tavicího procesu skel zahrnují i prezentace koncentračních polí nehomogenit. Kromě kinetiky chování jednotlivých nehomogenit v tavenině je tedy třeba uvažovat i jejich distribuci v daném tavicím prostoru. Tato práce představuje tři distribuční modely nutné pro modelování procesu odstraňování bublin a pro řízení kvality tavených skel z hlediska této nehomogenity: distribuční model složek oxidačně-redukčních reakcí a dva modely distribuce částic (bubliny, pevné částice) v tavicím prostoru. V práci se diskutuje použitelnost jednotlivých modelů a jsou zde uvedeny příklady jejich aplikace. Článek rovněž popisuje metody a postupy pro získávání dat do prezentovaných modelů.